AMERICAN SOCIETY FOR MICROBIOLOGY | Journal of Virology®

VIRUS-CELL INTERACTIONS

The Viral ORF3 Protein Is Required for Hepatitis E Virus Apical Release and Efficient Growth in Polarized Hepatocytes and Humanized Mice

Gulce Sari,[a] Jingting Zhu,[b] Charuta Ambardekar,[b] Xin Yin,[b*] Andre Boonstra,[a] Zongdi Feng,[b,c] Thomas Vanwolleghem[a,d,e]

[a]Department of Gastroenterology and Hepatology, Erasmus University Medical Center, Rotterdam, The Netherlands
[b]Center for Vaccines and Immunity, The Research Institute at Nationwide Children's Hospital, Columbus, Ohio, USA
[c]Department of Pediatrics, The Ohio State University College of Medicine, Columbus, Ohio, USA
[d]Laboratory of Experimental Medicine and Pediatrics, Faculty of Medicine and Health Sciences, University of Antwerp, Antwerp, Belgium
[e]Department of Gastroenterology and Hepatology, Antwerp University Hospital, Antwerp, Belgium

Gulce Sari and Jingting Zhu contributed equally to this work. The order of names was determined alphabetically.

ABSTRACT Hepatitis E virus (HEV), an enterically transmitted RNA virus, is a major cause of acute hepatitis worldwide. Additionally, HEV genotype 3 (gt3) can frequently persist in immunocompromised individuals with an increased risk for developing severe liver disease. Currently, no HEV-specific treatment is available. The viral open reading frame 3 (ORF3) protein facilitates HEV egress *in vitro* and is essential for establishing productive infection in macaques. Thus, ORF3, which is unique to HEV, has the potential to be explored as a target for antiviral therapy. However, significant gaps exist in our understanding of the critical functions of ORF3 in HEV infection *in vivo*. Here, we utilized a polarized hepatocyte culture model and a human liver chimeric mouse model to dissect the roles of ORF3 in gt3 HEV release and persistent infection. We show that ORF3's absence substantially decreased HEV replication and virion release from the apical surface but not the basolateral surface of polarized hepatocytes. While wild-type HEV established a persistent infection in humanized mice, mutant HEV lacking ORF3 (ORF3null) failed to sustain the infection despite transient replication in the liver and was ultimately cleared. Strikingly, mice inoculated with the ORF3null virus displayed no fecal shedding throughout the 6-week experiment. Overall, our results demonstrate that ORF3 is required for HEV fecal shedding and persistent infection, providing a rationale for targeting ORF3 as a treatment strategy for HEV infection.

IMPORTANCE HEV infections are associated with significant morbidity and mortality. HEV gt3 additionally can cause persistent infection, which can rapidly progress to liver cirrhosis. Currently, no HEV-specific treatments are available. The poorly understood HEV life cycle hampers the development of antivirals for HEV. Here, we investigated the role of the viral ORF3 protein in HEV infection in polarized hepatocyte cultures and human liver chimeric mice. We found that two major aspects of the HEV life cycle require ORF3: fecal virus shedding and persistent infection. These results provide a rationale for targeting ORF3 to treat HEV infection.

KEYWORDS hepatitis E virus, ORF3, enteric viral hepatitis, interferon responses, human liver chimeric mice, polarized hepatocytes, vectorial release

Hepatitis E virus (HEV) is a single-stranded RNA virus belonging to the *Hepeviridae* family (1). HEV infects approximately 20 million people annually and is a major cause of acute viral hepatitis globally (2). Chronic HEV infection, mostly due to zoonotic

Citation Sari G, Zhu J, Ambardekar C, Yin X, Boonstra A, Feng Z, Vanwolleghem T. 2021. The viral ORF3 protein is required for hepatitis E virus apical release and efficient growth in polarized hepatocytes and humanized mice. J Virol 95:e00585-21. https://doi.org/10.1128/JVI.00585-21.

Editor J.-H. James Ou, University of Southern California

Address correspondence to Zongdi Feng, Zongdi.feng@nationwidechildrens.org, or Thomas Vanwolleghem, Thomas.Vanwolleghem@uza.be.

*Present address: Xin Yin, Harbin Veterinary Research Institute, Chinese Academy of Agricultural Sciences, Harbin, Heilongjiang, China.

Received 5 April 2021
Accepted 9 September 2021
Accepted manuscript posted online 15 September 2021
Published 9 November 2021

transmission of genotype 3 (gt3) HEV, is an emerging health problem in Western countries and can rapidly progress to liver cirrhosis within 2 to 3 years (3). Currently, no HEV-specific treatments are available. While ribavirin, a nucleoside analog, has been used successfully as an off-label drug to treat certain patients with chronic HEV infection, its associated side effects and viral resistance limit its use (4).

The poorly understood HEV infectious cycle is a major barrier to developing HEV-specific antivirals. HEV has a unique infectious cycle. The virus is shed into feces as non-enveloped particles but circulates in the bloodstream in a quasi-enveloped form (eHEV) (5). The infectivity of eHEV particles in patient serum or produced from cell culture is reduced compared to that of stool-derived or cell lysate-derived naked HEV particles (6, 7). Therefore, while it has been proposed that eHEV particles mediate virus spread in the liver (8), the precise mechanism of HEV spread *in vivo* remains unclear.

The viral open reading frame 3 (ORF3) protein has a significant role in eHEV biogenesis (8–12). Specifically, ORF3 interacts through a C-terminal PSAP late domain motif of the cellular endosomal sorting complex required for transport (ESCRT) machinery and promotes HEV envelopment and exit via the exosome pathway (9, 13). eHEV particles in the culture supernatant and the patient's serum both contain ORF3 (11, 14). ORF3 is also a viroporin, and introducing mutations that disrupt its ion channel activity reduces virion secretion (12). In addition to its role in HEV egress, ORF3 interacts with various host proteins (15–21) and modulates cellular pathways, including the interferon (IFN) pathway (22–25). Importantly, a mutant HEV lacking ORF3 failed to establish a productive infection in experimentally inoculated macaques (26).

Despite these advances, the exact functions of ORF3 in natural HEV infections remain poorly defined. Hepatocytes are highly polarized *in vivo*, with their apical membranes abutting the bile canaliculi and their basolateral membranes facing the sinusoid blood (27). A recent study by Capelli et al. demonstrated that HEV virions released from both the apical and basolateral surfaces of polarized F2 cells (a subclone of HepG2 cells) are enveloped (28). However, whether ORF3 is required for HEV release from either one or both sides remains uncertain. Of note, ORF3 primarily localizes to the apical membranes in HEV-infected F2 cells, and the vast majority (>96%) of progeny virus is released apically (28). These results imply that ORF3 facilitates HEV release primarily (if not exclusively) at the apical surface and raise questions about the role of ORF3 in HEV's basolateral release and how eHEV particles circulating in a patient's serum incorporate ORF3.

Although a previous study demonstrated the essential role of ORF3 *in vivo* (26), specific defects associated with the ORF3-deficient mutant have not been identified. In that study, *in vitro* transcripts of a wild-type (WT) or ORF3-deficient HEV genome (gt1; Sar-55 strain) were injected intrahepatically into two macaques, and signs of infection (viremia, serum alanine aminotransferase [ALT] elevation, and seroconversion) were monitored weekly in serum samples. Both macaques inoculated with ORF3-deficient transcripts exhibited no signs of infection. Importantly, as no liver, bile, or fecal samples were analyzed in that study, little is known with regard to the specific defect(s) *in vivo* in the absence of ORF3.

To address these critical gaps, we created an ORF3-deficient mutant (ORF3null) using a gt3 HEV infectious clone (Kernow C1/p6) as a backbone and compared it with WT HEV in their replication kinetics and release in both polarized F2 cell culture and human liver chimeric mice. Our results indicate that ORF3 is essential for efficient replication and apical (but not basolateral) HEV release. Mice inoculated with the ORF3null virus showed no fecal virus shedding despite evidence for intrahepatic replication. Further analysis revealed that both WT and ORF3null HEV induced a transient interferon response that may have contributed to the clearance of the ORF3null virus. Overall, these results shed new light on ORF3's functions *in vivo* and provide a rationale for targeting ORF3 as a novel strategy for treating HEV infection.

RESULTS

ORF3 is required for efficient growth of HEV in polarized hepatocytes. To investigate the role of ORF3 in HEV replication, we replaced the start codon of ORF3 with

GCA in the gt3 Kernow C1/p6 strain to create a mutant HEV lacking ORF3 expression (ORF3null). *In vitro*-transcribed WT or ORF3null HEV RNA was transfected into HepG2/C3A cells. Five days later, cells were lysed and examined for ORF2 (capsid) or ORF3 protein expression by Western blotting. WT HEV RNA-transfected cells and ORF3null RNA-transfected cells had comparable levels of the ORF2 protein, which is translated from the same subgenomic RNA as ORF3 is. However, ORF3 was detected only in cells transfected with WT HEV RNA (Fig. 1A).

We then purified nonenveloped HEV virions from WT and ORF3null RNA-transfected cells and compared their specific infectivities in F2 cells (a subclone of HepG2/C3A cells). We used an immunofluorescence assay (IFA) with an antibody specific for ORF2 to quantify the number of focus-forming units (FFU) at 5 days postinoculation (dpi). We found that WT and ORF3null virions had similar specific infectivities (ratios of viral genome equivalents [GE] to FFU) (Fig. 1B). These results are in agreement with a previous study demonstrating that ORF3 is not essential for HEV replication and infectious particle production (29).

Next, we compared the growth of the WT and ORF3null HEV in polarized F2 cells (28). Polarization was achieved by growing the cells on a semipermeable membrane in the presence of 1% dimethyl sulfoxide (DMSO) for about 2 weeks. The intactness of the tight junctions was confirmed by measuring the transepithelial electrical resistance (TEER) (Fig. 1C) and permeability to fluorescein isothiocyanate (FITC)-conjugated dextran (molecular weight [MW] of 500 kDa) (Fig. 1D). We then inoculated polarized F2 cells with equal amounts of purified WT and ORF3null virions via the basolateral surface. Cells were fixed at 5 and 10 dpi and analyzed by an IFA with an anti-ORF2 antibody. These time points were chosen based on the replication kinetics of the Kernow C1/p6 strain in the HepG2/C3A cells, with a slow and gradual increase in the first 5 to 7 days followed by a steady level of persistent replication (30). No apparent cytotoxicity was detected during the course of the experiment as evidenced by minimal changes in the levels of lactate dehydrogenase (LDH) in the culture medium (Fig. 1E). Similar numbers of infected cells were detected for both viruses at 5 dpi, confirming that ORF3 is not required for infectivity. However, at 10 dpi, the number of infected cells increased for the WT virus but decreased for the ORF3null virus (Fig. 1F). Quantification of ORF2-positive areas from two independent experiments revealed a 2-fold increase during the period from 5 to 10 dpi in WT HEV-infected cells but a 4-fold decrease for ORF3null HEV-infected cells (Fig. 1G).

ORF3 is required for counteracting the HEV-induced interferon response. We have previously shown that HEV induces a type III IFN response that restricts virus replication (30). In addition, ORF3 has been shown to either enhance or block the IFN pathway (22, 23, 31). To investigate if IFN responses played a role in reducing the replication of the ORF3null virus beyond 5 days, we measured the expression of a panel of 3 IFN-stimulated genes (ISGs) 5, 7, 10, 12, and 15 days after virus inoculation. Consistent with the IFA results, intracellular HEV RNA levels were gradually increased in WT HEV-infected cells but were decreased in ORF3null HEV-infected cells (Fig. 1H). In contrast, the expression of all 3 ISGs (*ISG56*, *CXCL10*, and *ISG15*) was induced to higher levels in ORF3null HEV-infected cells than in WT HEV-infected cells (Fig. 1I).

Since ORF3 inhibits STAT1 activation (22), we investigated if blocking STAT1 function could rescue the ORF3-null virus replication. Treatment of cells with a Janus kinase inhibitor (JAKi) resulted in an increase in the replication of both WT and ORF3null viruses, but the effect was more profound for the ORF3null virus (Fig. 1F and G). Compared with the untreated group, there was a 3.8-fold increase in ORF2-positive areas in WT HEV-infected cells. However, a 10-fold increase was detected in ORF3null HEV-infected cells. Thus, the lower virus replication of the ORF3null virus likely resulted from a higher IFN response, its increased susceptibility to IFNs, or both.

Ectopically expressed ORF3 rescues the growth of the ORF3null virus. We determined if ectopically expressed ORF3 can rescue ORF3null virus replication by creating a cell line that stably expressed the ORF3 protein (F2-ORF3). The expression of ORF3 was confirmed by an IFA using an antibody specific for ORF3 (Fig. 2A). Parental F2 cells and cells transduced with an empty vector (F2-empty) served as controls. Cells were polarized in the transwell and inoculated with either WT or ORF3null HEV. At 5 and 10 dpi, cells

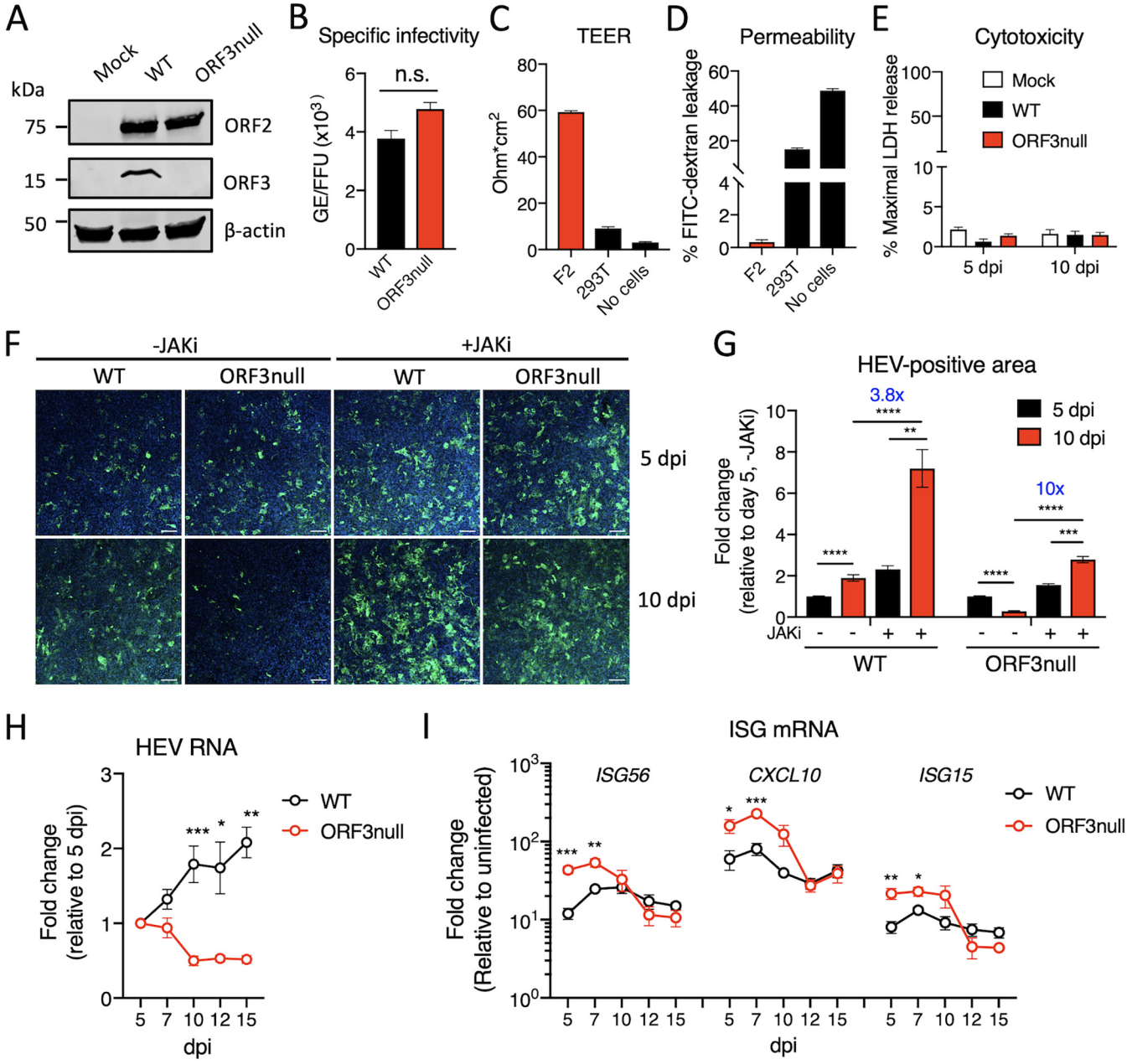

FIG 1 ORF3 is required for efficient HEV growth in polarized human hepatocytes. (A) Western blots of HEV ORF2 and ORF3 proteins in HepG2/C3A cells 5 days after transfection with wild-type (WT) or ORF3null HEV RNA. β-Actin served as the loading control. (B) Specific infectivity of WT and ORF3null virions recovered from HEV RNA-transfected cells. HEV genome equivalents (GE) were determined by qRT-PCR. ORF2-positive focus-forming units (FFU) were determined in F2 cells (a subclone of HepG2/C3A cells) by immunofluorescence assays at 5 days postinoculation. n.s., not significant. (C and D) Transepithelial electrical resistance (TEER) (C) and permeability (D) of F2 or 293T cells grown on a porous membrane (pore size, 3 μm) for 18 days. Data are shown as means $\pm$ standard errors of the means (SEM) from 2 independent experiments, each with duplicate wells. (E) Polarized F2 cells were inoculated with WT or ORF3null HEV (10^3 GE per cell). Lactate dehydrogenase (LDH) levels in the basolateral culture medium were measured at 5 and 10 days postinoculation (dpi). Data are shown as means $\pm$ SEM from triplicate wells. (F) Immunofluorescence images showing HEV ORF2-positive cells (green) in polarized F2 cell cultures 5 and 10 days after infection with WT or ORF3null HEV (10^3 GE per cell) in either the presence or absence of a JAK inhibitor (JAKi) (0.5 μM). Nuclei were counterstained with DAPI. Bars, 100 μm. (G) HEV-positive areas at 5 and 10 dpi were quantified using ImageJ software (NIH). Data are shown as means $\pm$ SEM from at least 2 independent experiments, each with duplicate wells. (H and I) Polarized F2 cells were inoculated with WT or ORF3null HEV (10^3 GE per cell), and the levels of HEV RNA (H) and interferon-stimulated genes (ISGs) (I) were quantified by qRT-PCR at the indicated times. Data are shown as means $\pm$ SEM from 2 independent experiments, each with duplicate wells. *, $P < 0.05$; **, $P < 0.01$; ***, $P < 0.001$; ****, $P < 0.0001$.

were fixed and stained with an anti-ORF2 antibody, and ORF2-positive areas were quantified by ImageJ software. As expected, WT HEV-infected parental F2 cells and F2-empty cells showed an increase in ORF2-positive areas from 5 dpi to 10 dpi, while ORF3null virus-infected cells showed a decrease (Fig. 2B). Overexpression of ORF3 did not further increase

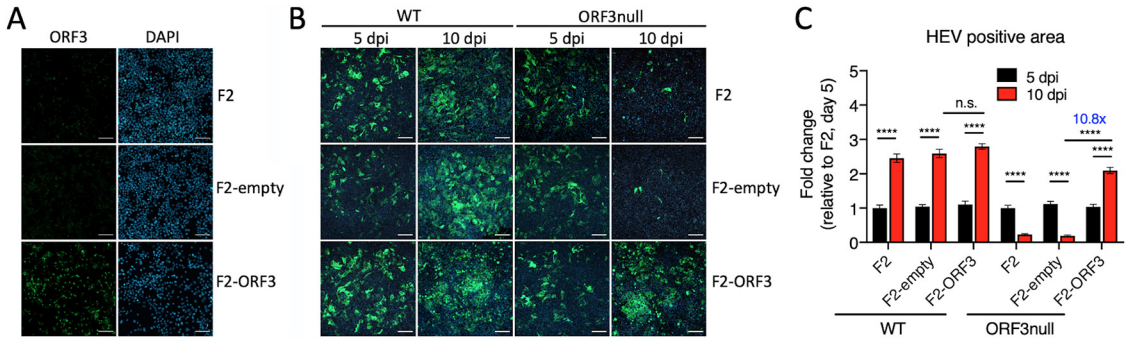

FIG 2 Overexpressed ORF3 protein rescues the growth of ORF3null HEV in polarized human hepatocytes. (A) Immunofluorescence images showing ORF3-positive cells (green) in F2 (a subclone of HepG2/C3A cells), F2-empty (F2 cells transduced with an empty lentiviral vector), and F2-ORF3 (F2 cells transduced with an ORF3-expressing lentiviral vector) cells. Nuclei were stained with DAPI. Bars, 100 μm. (B) Immunofluorescence images showing HEV ORF2-positive cells (green) in polarized F2, F2-empty, and F2-ORF3 cells 5 and 10 days after infection with WT or ORF3null HEV (10^3 GE per cell). Bars, 100 μm. (C) HEV-positive areas at 5 and 10 days postinfection (dpi) were quantified using ImageJ software (NIH). Data are shown as means ± SEM from triplicate wells. n.s., not significant; ****, $P < 0.0001$.

WT HEV replication. However, it significantly enhanced the growth of the ORF3null virus; ORF2-positive areas in F2-ORF3 cells at 10 dpi had an approximately 10-fold increase over those in the parental F2 cells and the F2-empty cells (Fig. 2C). Thus, the ectopic expression of ORF3 can effectively rescue the growth of the ORF3null virus.

ORF3 promotes the apical release of HEV from polarized hepatocytes. Previous studies have shown that ORF3 promotes HEV release (8–12). However, the role of ORF3 in HEV release from polarized hepatocytes is unknown. To address this question, we inoculated polarized F2 cells with either WT or ORF3null HEV. After 7 days, HEV RNA in culture supernatants collected from the top (apical) and bottom (basolateral) chambers of the transwells as well as intracellular HEV RNA were extracted and quantified by real-time PCR. This analysis revealed that while WT HEV was primarily released apically, ORF3null HEV was released almost equally to the apical and basolateral compartments (Fig. 3A). After adjusting to the intracellular HEV RNA levels, ORF3null HEV showed an ~70% reduction in apical release compared to WT HEV (Fig. 3B). However, basolateral HEV release was not affected in the absence of ORF3 (Fig. 3C). Infectivity assays confirmed that infectious virus was mainly released apically for WT HEV but was released in similar quantities to the apical and basolateral compartments for ORF3null HEV (Fig. 3D and E). Corroborating these findings, the ORF3 protein was detected almost exclusively in the apical compartment (Fig. 3F). The secreted ORF2 protein, which is released via the secretory pathway (32), was detected in similar quantities in the apical and basolateral compartments.

Importantly, the ectopic expression of ORF3 rescued the apical release of the ORF3null virus (Fig. 3G to I). The overexpression of ORF3 also slightly increased the release of WT HEV, but the extents of the increase were similar in the apical and basolateral compartments (Fig. 3H and I).

ORF3 is required for HEV fecal shedding and sustained replication in the liver of humanized mice. We previously demonstrated that HEV can establish persistent infections in human liver chimeric mice, independent from the mouse genetic background (6, 33). To extend our observations in F2 cells and further investigate the role of ORF3 for HEV release in the biliary tract *in vivo*, we compared the kinetics of WT and ORF3null viruses in different compartments of humanized mice with optimal human hepatocyte engraftment (serum human albumin levels of >100 μg/ml) (33). In the first experiment, we intravenously inoculated humanized mice with 10^6 GE of either WT ($n = 5$) or ORF3null ($n = 3$) HEV and collected blood (biweekly) and feces (weekly) for 6 weeks, at which time animals were sacrificed to analyze HEV RNA and antigens in liver and bile (Fig. 4A). Continuous fecal virus shedding was observed for the WT HEV-inoculated group (Fig. 4B). In contrast, mice inoculated with the ORF3null virus had no detectable fecal shedding at all time points.

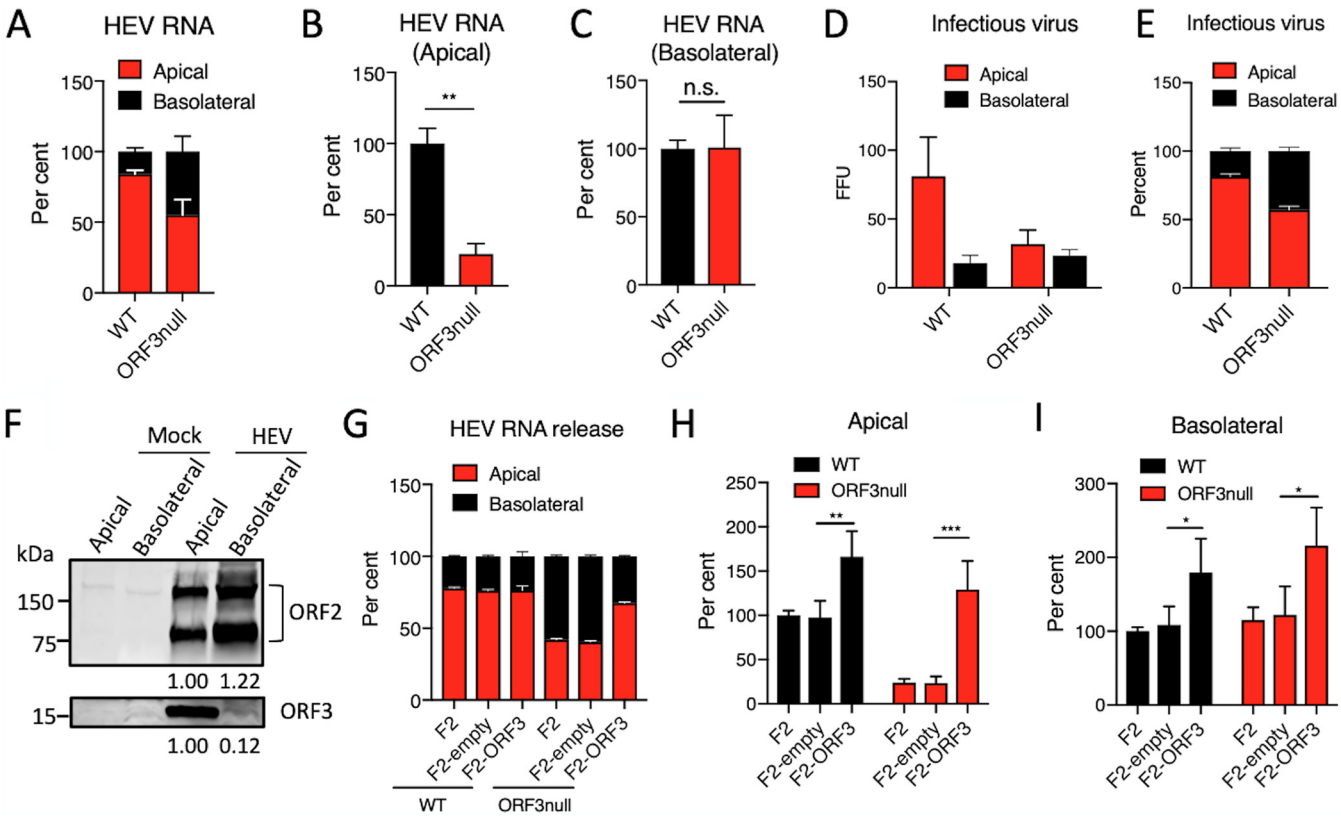

FIG 3 ORF3 facilitates apical release of HEV particles from polarized human hepatocytes. (A to C) Polarized F2 cells were inoculated with WT or ORF3null HEV (5×10^3 GE per cell). After 7 days, HEV RNA in the culture supernatants from the top (apical) and lower (basolateral) chambers and intracellular HEV RNA were isolated and quantified by qRT-PCR. (A) Relative amounts of HEV RNA present in the supernatants from the apical versus basolateral chambers. (B and C) Relative amounts of WT versus ORF3null HEV RNA present in the apical (B) and basolateral (C) chambers (extracellular HEV RNA levels were normalized to intracellular HEV RNA levels to adjust the difference in virus replication between WT and ORF3null HEV, and the values from the WT HEV-infected group were set as 100%). Data are shown as means ± SEM from at least 2 independent experiments, each with duplicate wells. n.s., not significant; **, $P < 0.01$. (D and E) Polarized F2 cells were inoculated with WT or ORF3null HEV (5×10^3 GE per cell), and culture supernatants in the apical and basolateral chambers were collected at 5 dpi to inoculate naive F2 cells. (D) Cells were fixed 5 days later, and ORF2-positive focus-forming units (FFU) were determined by immunofluorescence assays. (E) Relative amounts of infectious virus present in the apical versus basolateral compartments. Data are shown as means ± SEM from triplicate samples. (F) Western blots of ORF2 and ORF3 proteins in culture supernatants from the apical and basolateral chambers of WT HEV (5×10^3 GE per cell)-infected polarized F2 cell cultures. Note that the secreted ORF2 protein existed in both monomeric and dimeric forms. Values below each blot indicate the relative ORF2 or ORF3 protein levels. (G to I) Polarized F2, F2-empty, and F2-ORF3 cells were inoculated with WT or ORF3null HEV (5×10^3 GE per cell). After 7 days, HEV RNAs in culture supernatants (in both the apical and basolateral chambers) and cells were isolated and quantified by qRT-PCR. (G) Relative amounts of HEV RNA present in the supernatants from the apical versus the basolateral chambers. (H and I) Relative amounts of WT versus ORF3null HEV RNA released in the apical (H) and basolateral (I) chambers (values from WT-infected F2 cells were set as 100%). Data are shown as means ± SEM from 2 independent experiments, each with duplicate wells. *, $P < 0.05$; **, $P < 0.01$; ***, $P < 0.001$.

Low levels of HEV RNA were also detected in the serum samples from mice inoculated with WT HEV but not in those inoculated with ORF3null HEV (Fig. 4B). High levels of HEV RNA were detected in the liver and bile of WT-infected mice but not in ORF3null-infected mice at week 6 (Fig. 4B). In addition, abundant HEV ORF2 proteins were detected in liver sections from WT HEV-infected mice at week 6 (Fig. 4C). Interestingly, despite the lack of detectable HEV RNA in ORF3null HEV-inoculated mice, ORF2 proteins were also detected in liver sections but at a much lower level.

Since we did not detect fecal virus shedding in the ORF3null HEV-inoculated group even as early as 1 week postinoculation, in the next experiment, we inoculated 3 humanized mice with 10^6 GE of the ORF3null virus and sacrificed them after 3 days. Again, the fecal materials had no detectable HEV RNA. However, abundant HEV RNA and antigen were detected in the liver (Fig. 4D and E). These results suggested that while the ORF3null virus replicated in the liver (by day 3), it could not be shed into the feces.

To further investigate the replication kinetics of the ORF3null virus in this model, we inoculated humanized mice with the ORF3null virus and sacrificed one animal at each time point, as indicated in Fig. 4F, excepting day 7 ($n = 2$). For comparison, 3

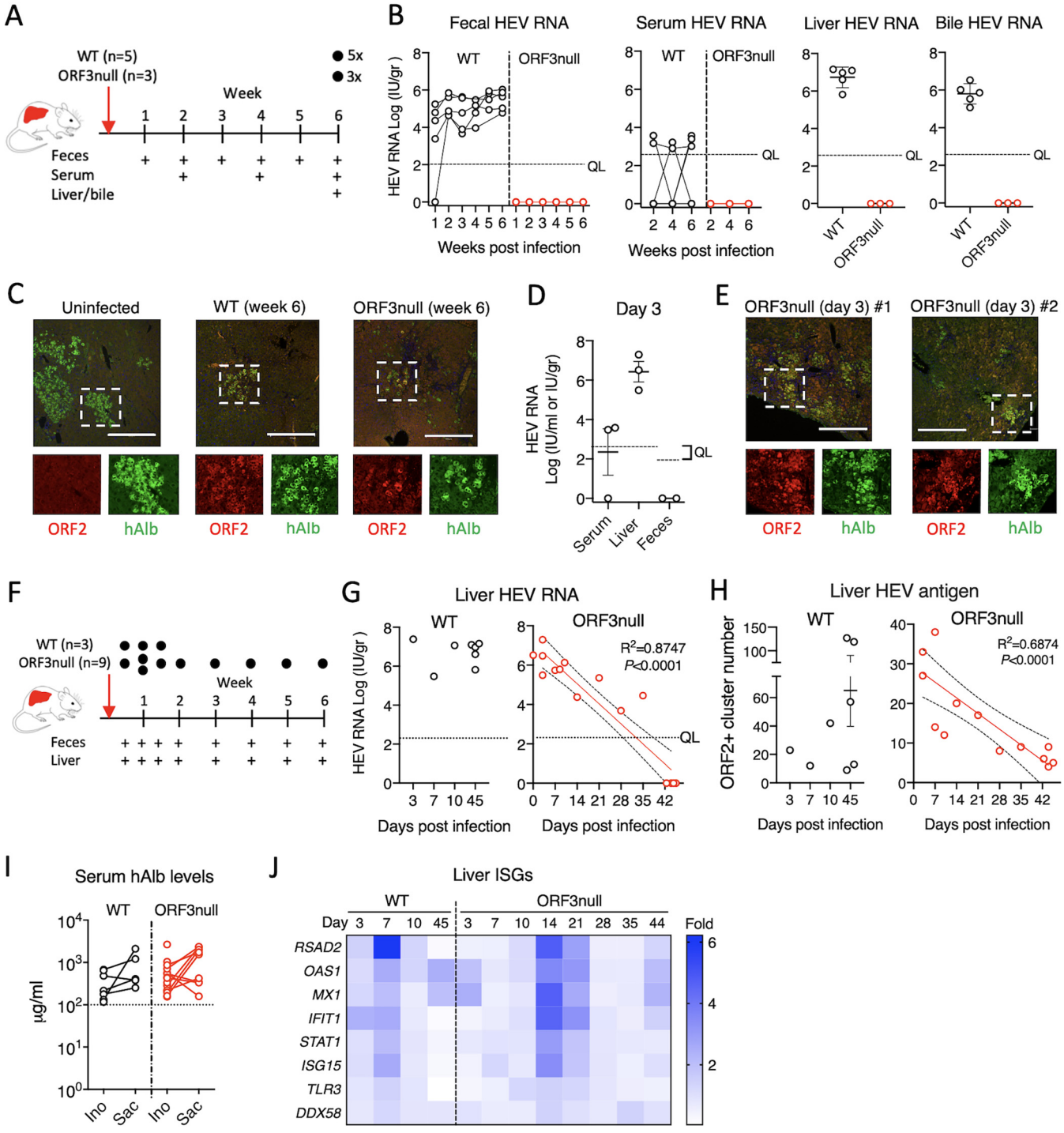

FIG 4 ORF3 is essential for HEV fecal shedding and persistent infection in humanized mice. (A to C) Human liver chimeric mice were inoculated with equal amounts (10^6 GE) of WT (n = 5) or ORF3null (n = 3) HEV. Serum samples were collected biweekly, and feces were collected weekly. Mice were sacrificed 6 weeks after virus inoculation. (B) HEV RNA levels in feces and serum at the indicated times and in liver and bile at week 6 were quantified by qRT-PCR. The dotted horizontal line indicates the quantification limit (QL). (C) Immunofluorescence images showing HEV ORF2 (red) and human albumin (hAlb) (green) in liver sections from HEV-infected humanized mice 6 weeks after inoculation. Bars, 450 μm. (D and E) Humanized mice were inoculated with the ORF3null virus (n = 3) and sacrificed 3 days after virus inoculation. (D) qRT-PCR-quantified HEV RNA levels in serum, liver, and feces 3 days after HEV inoculation. The dotted horizontal lines indicate the quantification limits. (E) Immunofluorescence images showing HEV ORF2 (red) and human albumin (green) in liver sections from two different ORF3null-infected mice. Bars, 450 μm. (F to H) Humanized mice were inoculated with equal amounts (10^6 GE) of WT (n = 3) or ORF3null (n = 9) HEV and sacrificed at the indicated times (black dots). (G and H) HEV RNA (G) and antigen (ORF2) (H) levels in the livers of humanized mice. Note that 5 additional WT-inoculated animals and a total of 6 additional ORF3null-inoculated animals (panels B and D) were also included for analyses in panels G and H. A downward trend in liver HEV RNA and antigen in the ORF3null-inoculated group is depicted with a linear regression fit (slope with 95% confidence intervals). (I) Serum human albumin levels in WT- and ORF3null-inoculated animals (panels A to H) at the time of HEV

(Continued on next page)

additional mice were inoculated with the WT virus to examine fecal shedding and liver titers at days 3, 7, and 10 postinoculation. Again, only WT-inoculated animals had detectable fecal virus shedding (data not shown). The liver HEV RNA titers were comparable between the two groups at early time points (3, 7, and 10 days) but decreased gradually in the ORF3null HEV-inoculated group and were undetectable at week 6 postinoculation (Fig. 4G). Immunofluorescence staining of liver sections with an anti-ORF2 antibody confirmed the decreasing HEV antigen levels in ORF3null virus-inoculated animals over 6 weeks (Fig. 4H). The lack of ORF3null virus replication was not due to insufficient humanization in these animals since numerous human cell islands were detected in the livers of ORF3null HEV-infected mice. Furthermore, the serum human albumin levels in ORF3null HEV-inoculated mice remained above the established 100-μg/ml cutoff for HEV permissiveness (33) (Fig. 4I). These results indicate that ORF3null virus replication gradually declined, and the virus was ultimately cleared from the liver.

Since humanized mice lacked adaptive immune responses and the results obtained from F2 cells suggested that IFN responses play a role in inhibiting ORF3null HEV replication, we examined the expression of a panel of human ISGs in longitudinally collected liver samples from WT HEV- or ORF3null HEV-inoculated animals. Both WT and ORF3null HEV induced transient ISG expression in the liver (Fig. 4J). There appeared to be a delay in the kinetics and a slight increase in the ISG response in the ORF3null HEV-inoculated group compared to the WT HEV-inoculated group. However, the number of animals was insufficient for statistical analysis.

DISCUSSION

This study aimed to better understand the function of ORF3 in the HEV infectious cycle. We used both a polarized hepatocyte culture and a human liver chimeric mouse model to examine the impact of ORF3 deletion on HEV growth and virion secretion. Our study revealed two major findings. First, deleting ORF3 significantly impaired virus release from the apical surface of human hepatocytes. This impairment was evidenced by a 70% reduction in apical virus release from polarized F2 cells and a complete lack of fecal virus shedding from humanized mice in the absence of ORF3. Second, deleting ORF3 impaired HEV growth both in F2 cells and in humanized mice. The ORF3null virus was ultimately cleared in the liver, in contrast to the WT virus, which persisted for the entire 6-week experiment. The reduced growth in the absence of ORF3 was accompanied by an enhanced IFN response *in vitro*, and inhibiting the IFN response by a JAK inhibitor rescued ORF3null virus replication. Taken together, our findings demonstrate two essential functions of ORF3 in the HEV life cycle: (i) promoting the release of progeny virus from the apical/canalicular membrane of HEV-infected hepatocytes and (ii) facilitating HEV replication in part by counteracting intracellular IFN responses.

The complete lack of fecal virus shedding in the absence of ORF3 is a remarkable finding. Notably, fecal virus shedding was not observed in ORF3null-inoculated animals even at very early time points (days 3, 7, and 10) when abundant HEV RNA and antigen were readily detectable in the liver, indicating that this defect was not due to insufficient virus replication. This finding concurs with ORF3 localizing primarily to the apical membranes (34–36), the vast majority of ORF3 protein being secreted apically, and a 70% reduction in apical virus release from polarized F2 cells in the absence of ORF3. The N terminus of ORF3 has a highly conserved palmitoylation signal, which, when disrupted, resulted in a loss of ORF3 membrane association and impaired HEV release (37). Thus, palmitoylation may play a role in targeting ORF3 to the apical membranes in HEV-infected hepatocytes. It will be interesting to test if ORF3 palmitoylation is required for HEV apical release and fecal shedding in future work.

FIG 4 Legend (Continued)
inoculation (Ino) and at sacrifice (Sac). The dotted horizontal line indicates the established cutoff value for WT HEV permissiveness in humanized mice. (J) Heat map of intrahepatic ISG expression in HEV-inoculated humanized mice. Data are shown as mean fold changes relative to uninfected controls (n = 4). The numbers of animals included for analyses are as follows: 1 mouse for days 3, 7, and 10 and 3 mice for day 45 for the WT group and 1 mouse for days 10, 14, 21, 28, and 35; 3 mice for day 3; 2 mice for day 7; and 4 mice for day 44 for the ORF3null group.

Unexpectedly, we found that the basolateral release of HEV was unaffected. Almost equal amounts of HEV were detected in the apical and basolateral sides of ORF3null-infected polarized F2 cells. Also, the absence of ORF3 did not affect the ratio of basolaterally released HEV to intracellular HEV. Unfortunately, since only very low levels of HEV RNA were detected in sera in our humanized mouse model, it was not possible to assess the impact of ORF3 deletion on basolateral HEV secretion in this model. Nonetheless, these *in vitro* results challenge the existing model that eHEV biogenesis requires ORF3 and contradicts the fact that circulating eHEV particles contain ORF3 (14). ORF3 can interact with the ESCRT protein Tsg101 and promote HEV budding into the multivesicular bodies (MVBs), and fusion of the MVBs with the plasma membrane results in the release of single-membrane-encased eHEV particles (10, 13). Furthermore, in HEV-infected nonpolarized cells, both ORF2 and ORF3 colocalize with CD63, a marker of MVBs (13). However, in polarized hepatocytes and humanized mice, ORF3 primarily localizes to the apical membranes rather than the internal membranes (28, 34), which coincides with our results indicating that ORF3 was released almost exclusively at the apical surface. In future work, it will be interesting to test if blocking the ORF3-ESCRT interaction results in impairments in HEV release at the apical or basolateral side, or both, in polarized hepatocyte cultures and *in vivo*.

Another striking finding is the requirement of ORF3 for efficient HEV growth in polarized F2 cells. This result contradicts a previous report by Shukla et al. where HEV spread in HepG2/C3A cells did not require ORF3 (38). As discussed above, HEV spread and infection outcomes in nonpolarized cells cannot be compared to results obtained in differentiated polarized hepatocytes. Furthermore, different methods were used. In the study by Shukla et al., *in vitro*-transcribed HEV RNAs were electroporated into HepG2/C3A cells, and infection was monitored by flow cytometry. Infection may be advantageous over electroporation due to minimal toxicity and a synchronized low multiplicity of infection, both of which are necessary for studying virus spread. Besides, in our experience, HEV infection caused changes in the cell morphology over time, resulting in a shift in the cell population on the scatterplots. Thus, flow cytometry results should be interpreted with caution and preferably confirmed by independent assays.

Finally, we observed a slight increase in the HEV-induced IFN response in the absence of ORF3. ORF3 can either enhance IFN production or inhibit IFN signaling (22, 23). Therefore, the interplay between ORF3 and the IFN pathway in HEV-infected polarized hepatocytes merits further study.

In summary, our study demonstrates that ORF3 is required for HEV apical release and efficient growth in polarized hepatocytes and for fecal virus shedding and persistent infection in humanized mice. These results provide a rationale for targeting ORF3 as a strategy for treating HEV infection.

MATERIALS AND METHODS

Cells and viruses. S10-3 (a subclone of Huh-7 cells provided by Suzanne Emerson), HEK293T, HepG2/C3A (ATCC CRL-10741), and F2 (a subclone of HepG2/C3A cells, provided by Jacques Izopet) cells were maintained in growth medium containing Dulbecco's modified Eagle medium (DMEM) supplemented with 10% fetal bovine serum (FBS) and 1% penicillin-streptomycin (pen-strep) (Fisher Scientific). Polarized F2 cells were obtained by culturing the cells on collagen-coated semipermeable transwell inserts (Corning) for 14 days at 37°C in William's medium E containing 10% FBS and 1% DMSO. Cell polarization was confirmed before each experiment by assessing the permeability of FITC-conjugated dextran (Invitrogen). A gt3a HEV strain (Kernow C1/p6; GenBank accession number JQ679013) was used as a backbone to construct the ORF3null virus. Briefly, the AflII and PmlI fragments from the infectious clone were excised and cloned into an intermediate vector. The start codon of ORF3 was mutated to GCA using an Agilent site-directed mutagenesis kit. After verifying the sequence, the AflII and PmlI fragments were excised and cloned back to the infectious clone. Plasmids containing the HEV genome were linearized with MluI, and full-length capped HEV genomes were synthesized using an mMessage mMachine T7 transcription kit (Thermo Fisher). Virus stocks were prepared by transfecting *in vitro* transcripts into S10-3 cells followed by gradient ultracentrifugation to purify intracellular nonenveloped virions as described previously (7).

Construction of ORF3-overexpressing cells. The ORF3 coding sequence from the HEV Kernow C1/p6 strain was cloned into the pHIV-dTomato vector (a gift from Bryan Welm; Addgene plasmid 21374) to yield pHIV-dTomato-ORF3. 293T cells were transfected with pMD2.G, psPAX2, and pHIV-dTomato-ORF3 (or the empty pHIV-dTomato vector) at a 1:3:4 ratio using Lipofectamine 3000 (Thermo Fisher Scientific, Inc.). Supernatants containing packaged lentivirus were harvested at 72 h posttransfection, centrifuged

at 500 × *g* for 3 min, filtered through a 0.45-μm filter, and used to inoculate F2 cells in the presence of 8 μg/ml Polybrene (Sigma-Aldrich). The transduction efficiency was determined by dTomato expression in the transduced cells.

Virus infection. HEV (1×10^3 or 5×10^3 genome equivalents [GE] per cell) was added to the basolateral side of the polarized F2 cells, incubated at 34.5°C overnight, washed three times with phosphate-buffered saline (PBS), refed with hepatocyte maintenance medium (HMM) (catalog number Y30051; TaKaRa Bio), and cultured at 34.5°C for the duration of the experiments. On day 5 and day 10 postinfection, cells were fixed and stained with a rabbit polyclonal antibody against HEV ORF2 protein (a gift from X. J. Meng at Virginia Tech). For JAK inhibitor treatment experiments, directly after HEV inoculation, cells were maintained in a culture medium containing 0.5 μM JAK inhibitor II (Sigma-Aldrich) for the duration of the experiments.

FITC-dextran permeability assay. The integrity of F2 cell monolayers grown in the transwell was assessed by measuring the permeability of FITC-conjugated dextran (MW of 500 kDa; Invitrogen) (39). Briefly, medium containing 100 mg/ml FITC-dextran was added to the apical side. After 1 h of incubation at 37°C, fluorescence signals in the basolateral fluid were measured with a Synergy 2 multimode microplate reader (Bio-Tek). The percentage of the input was obtained by dividing the amount of dextran detected in the basolateral fluid with the input amount.

TEER measurement. A total of 1.65×10^4 F2 cells or HEK293T cells were seeded and cultured on collagen-coated semipermeable transwell inserts (Corning) for 18 days. The transepithelial electrical resistance (TEER) was measured by using an epithelial voltohmmeter (EVOM; World Precision Instruments).

LDH cytotoxicity assay. Cell viability was assessed with an LDH-Glo cytotoxicity assay kit (Promega), which measures LDH activity released from the cytosol of damaged cells. Briefly, polarized F2 cells were inoculated with WT or ORF3null HEV. LDH activity in the basolateral culture medium was measured at 5 days and 10 days postinfection according to the manufacturer's protocol.

Western blot analysis. Cells were directly lysed in a lysis buffer (100 mM Tris-HCl [pH 7.5], 50 mM NaCl, 5 mM EDTA, and 1% Triton X-100 in the presence of a protease inhibitor cocktail [Roche]). To detect ORF2 and ORF3 proteins in the culture medium, supernatants collected from the apical and basolateral sides of HEV-infected polarized F2 cells were concentrated using a Vivaspin column (100-kDa MW cutoff [MWCO]; Sartorius). The concentrated medium was resuspended in a lysis buffer. Samples were boiled for 5 min, and proteins were separated on a 4 to 20% SDS-PAGE gel and blotted onto a polyvinylidene difluoride (PVDF) membrane for Western blot analysis using a murine monoclonal antibody against HEV ORF2 (catalog number MAB8002; MilliporeSigma), a rabbit polyclonal antibody against HEV ORF3 (catalog number BS-0212R; Bioss USA), and a murine anti-β-actin antibody (catalog number A2228; MilliporeSigma).

Quantitative reverse transcription-PCR. Intracellular RNA was extracted with a QIAmini RNA isolation kit (Qiagen). HEV RNA in the culture supernatants was extracted with a QIAamp viral RNA isolation kit (Qiagen). HEV RNA was quantified by quantitative reverse transcription-PCR (qRT-PCR) using an iTaq universal probe one-step kit (Bio-Rad), using forward (F) primer HEV-F (5′-GGTGGTTTCTGGGGTGAC-3′), reverse (R) primer HEV-R (5′-AGGGGTTGGTTGGATGAA-3′), and probe HEV-P (5′-FAM [6-carboxyfluorescein]-TGATTCTCAGCCCTTCGC-TAMRA [6-carboxytetramethylrhodamine]-3′). HEV RNA levels in Fig. 3G to I were quantified by using forward primer HEV ORF1-F (5′-AAGACCTTCTGCGCTTTGTT-3′), reverse primer HEV ORF1-R (5′-TGACTCCTCATAAGCATCGC-3′), and probe HEV ORF1-P (5′-FAM-CCGTGGTTC CGTGCCATTGA-TAMRA-3′). Synthetic full-length HEV Kernow C1/p6 RNA served as the standard. Interferon-stimulated genes were quantified using an iTaq universal SYBR green one-step kit (Bio-Rad) with primers as described in our previous publication (30). The relative expression level was calculated using $2^{-\Delta CT}$ conversion. For intrahepatic ISG expression analysis, RNA was isolated using Qiazol (Qiagen, Hilden, Germany) from liver tissues stored in RNAlater (Qiagen, Hilden, Germany). cDNA was generated by using PrimeScript reverse transcriptase master mix (TaKaRa Bio, Inc., Kusatsu, Japan) according to the manufacturer's protocol. The ISG expression analysis used the following TaqMan probes: CXCL10 (catalog number Hs01124251_g1), DDX58 (Hs01061436_m1), IFIT1 (Hs01911452_s1), ISG15 (Hs01921425_s1), MX1 (Hs00895608_m1), OAS1 (Hs00973637_m1), RSAD2 (Hs00369813_m1), STAT1 (Hs01013996_m1), and Toll-like receptor 3 (TLR3) (Hs01551078_m1) (Life Technologies). Glyceraldehyde-3-phosphate dehydrogenase (GAPDH) (catalog number Hs00266705_g1) was used as a housekeeping gene control, and the relative expression level was calculated using $2^{-\Delta CT}$ conversion. The cross-reactivity of primers was checked using samples from C57BL/6 mice and nontransplanted NOG mice.

Mouse origin and *in vivo* infection experiments. Urokinase-type plasminogen activator (uPA) NOD/Shi-scid/IL-2Rγnull (NOG) and thymidine kinase (TK)-NOG mouse embryos were provided by H. Suemizu (Central Institute for Experimental Animals, Kawasaki, Japan) (40, 41). Mice were bred at the Central Animal Facility of the Erasmus Medical Center (DEC number 141-12-11), and offspring zygosity was determined using a copy number duplex quantitative PCR (qPCR) or custom-designed primer-probe mix (F primer CGATTCGCCGCGTTTACG, R primer CGCCGCCCTGCAGATA, and probe FAM-CCGCACCGTAT TGGCAA-BHQ1 [black hole quencher 1]) targeting the TK gene. Assays were performed on phenol-chloroform-isoamyl alcohol (Sigma-Aldrich, St. Louis, MO, USA)-extracted genomic mouse DNA from toe snips. TaqMan genotyping master mix (Life Technologies, Carlsbad, CA, USA), a TaqMan uPA genotyping assay (catalog number Mm00422051_cn; Life Technologies), and Tert gene reference mix (Life Technologies) were used according to the manufacturer's protocol. Homozygous $uPA^{+/+}$ or TK^{+} mice were anesthetized and transplanted with 0.5×10^6 to 2×10^6 viable commercially available cryopreserved human hepatocytes (Lonza, Basel, Switzerland [lot number 345], and Corning, Corning, NY, USA) via the intrasplenic injection route (42). At days −7 and −5 before transplantation, TK^{+} mice received an intraperitoneal ganciclovir injection to initiate liver damage (1). Hepatocyte engraftment levels were

determined in mouse sera using a human albumin enzyme-linked immunosorbent assay (ELISA) as previously described (Bethyl Laboratories, Montgomery, TX, USA) (6, 42). Successfully engrafted mice as defined by a serum human albumin level above the established cutoff of 100 μg/ml for HEV permissiveness (33) were intravenously inoculated with either 10^6 GE WT or ORF3null viruses. As *in vivo* HEV permissiveness is independent of the mouse genetic background once a minimal human chimerism level is reached, humanized uPA-NOG and TK-NOG mice with similar human albumin levels were included for these HEV infectivity studies. HEV RNA levels were determined using an ISO15189:2012-validated, internally controlled qRT-PCR in weekly collected fecal samples, biweekly collected serum samples, and liver and bile samples collected at sacrifice, as described previously (43).

Immunofluorescence assay and confocal microscopy. Liver tissues were fixed in 4% formaldehyde (Merck Millipore). For microscopy imaging, 4- to 5-μm cuts were prepared from paraffin-embedded blocks. Antigen was retrieved by heating the slides in a citrate buffer (Life Technology) at 98°C for 15 min. Liver sections were stained with a rabbit anti-ORF2 antibody at a 1:100 dilution (a gift from X. J. Meng at Virginia Tech) and a goat anti-human albumin antibody at a 1:200 dilution (catalog number A80-229A; Bethyl Laboratories) followed by Alexa Fluor 488- or 594-conjugated secondary antibodies at a 1:500 dilution (Thermo Fisher). Nuclei were counterstained with 4′,6-diamidino-2-phenylindole (DAPI) (Thermo Fisher). Slides were viewed with an EVOS fluorescence microscope (Thermo Fisher). In the confocal microscopy experiment, on day 5 and day 10 postinfection, cells were fixed with 4% paraformaldehyde and permeabilized with 0.2% Triton X-100 in PBS, followed by staining with a rabbit polyclonal anti-HEV ORF2 antibody (1:100 dilution) and an Alexa Fluor 488-conjugated secondary antibody (1:500 dilution). Cells were viewed with a Zeiss LSM 800 confocal laser scanning microscope. Images were acquired using ZEN 2009 software. HEV ORF2-positive areas were quantified using ImageJ software (NIH). Briefly, images were changed to 8-bit, and a threshold was selected and applied to all images in the same experiment to identify positive areas.

Statistical analysis. Statistical significance was assessed by unpaired *t* tests and linear regression in GraphPad Prism 8. Significance values are shown with asterisks in the figures (*, $P < 0.05$; **, $P < 0.01$; ***, $P < 0.001$; ****, $P < 0.0001$).

ACKNOWLEDGMENTS

We thank Suzanne Emerson, X. J. Meng, and Jacques Izopet for providing reagents; Jolanda J. Kreeft-Voermans for her support and supervision; and Claudia E. Mulders for technical assistance. We also thank Kubra Koten, who was involved in the initial studies.

The study was supported by the National Institute of Allergy and Infectious Diseases of the National Institutes of Health under award number R01AI139511 (Z.F.) and the Foundation for Liver and Gastrointestinal Research (SLO), Rotterdam, The Netherlands. T.V. is the recipient of a senior clinical research mandate from the Fund for Scientific Research (FWO), Flanders, Belgium (18B2821N). The funders had no role in study design, data collection and interpretation, and preparation of the manuscript.

Z.F. and T.V. conceived the study. G.S. performed the animal experiments and quantified the HEV RNA and ISG levels in tissues. J.Z. performed the cell culture experiments and liver tissue staining. C.A. prepared virus stocks and performed initial cell culture experiments. X.Y. constructed the ORF3null virus. G.S., J.Z., Z.F., and T.V. analyzed the data. A.B., Z.F., and T.V. supervised the study and acquired funding. T.V. acquired funding to establish the mouse model. G.S. and J.Z. wrote the draft, and Z.F. and T.V. edited the manuscript. All authors commented on the manuscript.

We declare no competing financial interests.

REFERENCES

1. Purdy MA, Harrison TJ, Jameel S, Meng X-J, Okamoto H, Van der Poel WHM, Smith DB, ICTV Report Consortium. 2017. ICTV virus taxonomy profile: Hepeviridae. J Gen Virol 98:2645–2646. https://doi.org/10.1099/jgv.0.000940.
2. World Health Organization. 2020. Hepatitis E: fact sheets. World Health Organization, Geneva, Switzerland.
3. Kamar N, Pischke S. 2019. Acute and persistent hepatitis E virus genotype 3 and 4 infection: clinical features, pathogenesis, and treatment. Cold Spring Harb Perspect Med 9:a031872. https://doi.org/10.1101/cshperspect.a031872.
4. Lhomme S, Marion O, Abravanel F, Izopet J, Kamar N. 2020. Clinical manifestations, pathogenesis and treatment of hepatitis E virus infections. J Clin Med 9:331. https://doi.org/10.3390/jcm9020331.
5. Feng Z, Hirai-Yuki A, McKnight KL, Lemon SM. 2014. Naked viruses that aren't always naked: quasi-enveloped agents of acute hepatitis. Annu Rev Virol 1:539–560. https://doi.org/10.1146/annurev-virology-031413-085359.
6. van de Garde MD, Pas SD, van der Net G, de Man RA, Osterhaus AD, Haagmans BL, Boonstra A, Vanwolleghem T. 2016. Hepatitis E virus (HEV) genotype 3 infection of human liver chimeric mice as a model for chronic HEV infection. J Virol 90:4394–4401. https://doi.org/10.1128/JVI.00114-16.
7. Yin X, Ambardekar C, Lu Y, Feng Z. 2016. Distinct entry mechanisms for nonenveloped and quasi-enveloped hepatitis E viruses. J Virol 90:4232–4242. https://doi.org/10.1128/JVI.02804-15.
8. Feng Z, Lemon SM. 2014. Peek-a-boo: membrane hijacking and the pathogenesis of viral hepatitis. Trends Microbiol 22:59–64. https://doi.org/10.1016/j.tim.2013.10.005.
9. Nagashima S, Takahashi M, Jirintai, Tanaka T, Yamada K, Nishizawa T, Okamoto H. 2011. A PSAP motif in the ORF3 protein of hepatitis E virus is necessary for virion release from infected cells. J Gen Virol 92:269–278. https://doi.org/10.1099/vir.0.025791-0.
10. Nagashima S, Takahashi M, Jirintai S, Tanaka T, Nishizawa T, Yasuda J, Okamoto H. 2011. Tumour susceptibility gene 101 and the vacuolar

protein sorting pathway are required for the release of hepatitis E virions. J Gen Virol 92:2838–2848. https://doi.org/10.1099/vir.0.035378-0.
11. Yamada K, Takahashi M, Hoshino Y, Takahashi H, Ichiyama K, Nagashima S, Tanaka T, Okamoto H. 2009. ORF3 protein of hepatitis E virus is essential for virion release from infected cells. J Gen Virol 90:1880–1891. https://doi.org/10.1099/vir.0.010561-0.
12. Ding Q, Heller B, Capuccino JM, Song B, Nimgaonkar I, Hrebikova G, Contreras JE, Ploss A. 2017. Hepatitis E virus ORF3 is a functional ion channel required for release of infectious particles. Proc Natl Acad Sci U S A 114:1147–1152. https://doi.org/10.1073/pnas.1614955114.
13. Nagashima S, Jirintai S, Takahashi M, Kobayashi T, Tanggis, Nishizawa T, Kouki T, Yashiro T, Okamoto H. 2014. Hepatitis E virus egress depends on the exosomal pathway, with secretory exosomes derived from multivesicular bodies. J Gen Virol 95:2166–2175. https://doi.org/10.1099/vir.0.066910-0.
14. Takahashi M, Yamada K, Hoshino Y, Takahashi H, Ichiyama K, Tanaka T, Okamoto H. 2008. Monoclonal antibodies raised against the ORF3 protein of hepatitis E virus (HEV) can capture HEV particles in culture supernatant and serum but not those in feces. Arch Virol 153:1703–1713. https://doi.org/10.1007/s00705-008-0179-6.
15. Zafrullah M, Ozdener MH, Panda SK, Jameel S. 1997. The ORF3 protein of hepatitis E virus is a phosphoprotein that associates with the cytoskeleton. J Virol 71:9045–9053. https://doi.org/10.1128/JVI.71.12.9045-9053.1997.
16. Korkaya H, Jameel S, Gupta D, Tyagi S, Kumar R, Zafrullah M, Mazumdar M, Lal SK, Xiaofang L, Sehgal D, Das SR, Sahal D. 2001. The ORF3 protein of hepatitis E virus binds to Src homology 3 domains and activates MAPK. J Biol Chem 276:42389–42400. https://doi.org/10.1074/jbc.M101546200.
17. Tyagi S, Surjit M, Roy AK, Jameel S, Lal SK. 2004. The ORF3 protein of hepatitis E virus interacts with liver-specific alpha1-microglobulin and its precursor alpha1-microglobulin/bikunin precursor (AMBP) and expedites their export from the hepatocyte. J Biol Chem 279:29308–29319. https://doi.org/10.1074/jbc.M402017200.
18. Tyagi S, Surjit M, Lal SK. 2005. The 41-amino-acid C-terminal region of the hepatitis E virus ORF3 protein interacts with bikunin, a Kunitz-type serine protease inhibitor. J Virol 79:12081–12087. https://doi.org/10.1128/JVI.79.18.12081-12087.2005.
19. Chandra V, Kalia M, Hajela K, Jameel S. 2010. The ORF3 protein of hepatitis E virus delays degradation of activated growth factor receptors by interacting with CIN85 and blocking formation of the Cbl-CIN85 complex. J Virol 84:3857–3867. https://doi.org/10.1128/JVI.01994-09.
20. Ratra R, Kar-Roy A, Lal SK. 2008. The ORF3 protein of hepatitis E virus interacts with hemopexin by means of its 26 amino acid N-terminal hydrophobic domain II. Biochemistry 47:1957–1969. https://doi.org/10.1021/bi7016552.
21. Ratra R, Kar-Roy A, Lal SK. 2009. ORF3 protein of hepatitis E virus interacts with the Bbeta chain of fibrinogen resulting in decreased fibrinogen secretion from HuH-7 cells. J Gen Virol 90:1359–1370. https://doi.org/10.1099/vir.0.009274-0.
22. Dong C, Zafrullah M, Mixson-Hayden T, Dai X, Liang J, Meng J, Kamili S. 2012. Suppression of interferon-α signaling by hepatitis E virus. Hepatology 55:1324–1332. https://doi.org/10.1002/hep.25530.
23. Nan Y, Ma Z, Wang R, Yu Y, Kannan H, Fredericksen B, Zhang YJ. 2014. Enhancement of interferon induction by ORF3 product of hepatitis E virus. J Virol 88:8696–8705. https://doi.org/10.1128/JVI.01228-14.
24. Chandra V, Kar-Roy A, Kumari S, Mayor S, Jameel S. 2008. The hepatitis E virus ORF3 protein modulates epidermal growth factor receptor trafficking, STAT3 translocation, and the acute-phase response. J Virol 82:7100–7110. https://doi.org/10.1128/JVI.00403-08.
25. Lei Q, Li L, Cai J, Huang W, Qin B, Zhang S. 2016. ORF3 of hepatitis E virus inhibits the expression of proinflammatory cytokines and chemotactic factors in LPS-stimulated human PMA-THP1 cells by inhibiting NF-kappaB pathway. Viral Immunol 29:105–111. https://doi.org/10.1089/vim.2015.0107.
26. Graff J, Nguyen H, Yu C, Elkins WR, St Claire M, Purcell RH, Emerson SU. 2005. The open reading frame 3 gene of hepatitis E virus contains a cis-reactive element and encodes a protein required for infection of macaques. J Virol 79:6680–6689. https://doi.org/10.1128/JVI.79.11.6680-6689.2005.
27. Treyer A, Musch A. 2013. Hepatocyte polarity. Compr Physiol 3:243–287. https://doi.org/10.1002/cphy.c120009.
28. Capelli N, Marion O, Dubois M, Allart S, Bertrand-Michel J, Lhomme S, Abravanel F, Izopet J, Chapuy-Regaud S. 2019. Vectorial release of hepatitis E virus in polarized human hepatocytes. J Virol 93:e01207-18. https://doi.org/10.1128/JVI.01207-18.
29. Emerson SU, Nguyen H, Torian U, Purcell RH. 2006. ORF3 protein of hepatitis E virus is not required for replication, virion assembly, or infection of hepatoma cells in vitro. J Virol 80:10457–10464. https://doi.org/10.1128/JVI.00892-06.
30. Yin X, Li X, Ambardekar C, Hu Z, Lhomme S, Feng Z. 2017. Hepatitis E virus persists in the presence of a type III interferon response. PLoS Pathog 13:e1006417. https://doi.org/10.1371/journal.ppat.1006417.
31. Lei Q, Li L, Zhang S, Li T, Zhang X, Ding X, Qin B. 2018. HEV ORF3 downregulates TLR7 to inhibit the generation of type I interferon via impairment of multiple signaling pathways. Sci Rep 8:8585. https://doi.org/10.1038/s41598-018-26975-4.
32. Yin X, Ying D, Lhomme S, Tang Z, Walker CM, Xia N, Zheng Z, Feng Z. 2018. Origin, antigenicity, and function of a secreted form of ORF2 in hepatitis E virus infection. Proc Natl Acad Sci U S A 115:4773–4778. https://doi.org/10.1073/pnas.1721345115.
33. Sari G, van Oord GW, van de Garde MDB, Voermans JJC, Boonstra A, Vanwolleghem T. 2021. Sexual dimorphism in hepatocyte xenograft models. Cell Transplant 30:9636897211006132. https://doi.org/10.1177/09636897211006132.
34. Allweiss L, Gass S, Giersch K, Groth A, Kah J, Volz T, Rapp G, Schobel A, Lohse AW, Polywka S, Pischke S, Herker E, Dandri M, Lutgehetmann M. 2016. Human liver chimeric mice as a new model of chronic hepatitis E virus infection and preclinical drug evaluation. J Hepatol 64:1033–1040. https://doi.org/10.1016/j.jhep.2016.01.011.
35. Emerson SU, Nguyen HT, Torian U, Burke D, Engle R, Purcell RH. 2010. Release of genotype 1 hepatitis E virus from cultured hepatoma and polarized intestinal cells depends on open reading frame 3 protein and requires an intact PXXP motif. J Virol 84:9059–9069. https://doi.org/10.1128/JVI.00593-10.
36. Dao Thi VL, Wu X, Belote RL, Andreo U, Takacs CN, Fernandez JP, Vale-Silva LA, Prallet S, Decker CC, Fu RM, Qu B, Uryu K, Molina H, Saeed M, Steinmann E, Urban S, Singaraja RR, Schneider WM, Simon SM, Rice CM. 2020. Stem cell-derived polarized hepatocytes. Nat Commun 11:1677. https://doi.org/10.1038/s41467-020-15337-2.
37. Gouttenoire J, Pollan A, Abrami L, Oechslin N, Mauron J, Matter M, Oppliger J, Szkolnicka D, Dao Thi VL, van der Goot FG, Moradpour D. 2018. Palmitoylation mediates membrane association of hepatitis E virus ORF3 protein and is required for infectious particle secretion. PLoS Pathog 14:e1007471. https://doi.org/10.1371/journal.ppat.1007471.
38. Shukla P, Nguyen HT, Faulk K, Mather K, Torian U, Engle RE, Emerson SU. 2012. Adaptation of a genotype 3 hepatitis E virus to efficient growth in cell culture depends on an inserted human gene segment acquired by recombination. J Virol 86:5697–5707. https://doi.org/10.1128/JVI.00146-12.
39. Hirai-Yuki A, Hensley L, Whitmire JK, Lemon SM. 2016. Biliary secretion of quasi-enveloped human hepatitis A virus. mBio 7:e01998-16. https://doi.org/10.1128/mBio.01998-16.
40. Hasegawa M, Kawai K, Mitsui T, Taniguchi K, Monnai M, Wakui M, Ito M, Suematsu M, Peltz G, Nakamura M, Suemizu H. 2011. The reconstituted 'humanized liver' in TK-NOG mice is mature and functional. Biochem Biophys Res Commun 405:405–410. https://doi.org/10.1016/j.bbrc.2011.01.042.
41. Suemizu H, Hasegawa M, Kawai K, Taniguchi K, Monnai M, Wakui M, Suematsu M, Ito M, Peltz G, Nakamura M. 2008. Establishment of a humanized model of liver using NOD/Shi-scid IL2Rgnull mice. Biochem Biophys Res Commun 377:248–252. https://doi.org/10.1016/j.bbrc.2008.09.124.
42. Vanwolleghem T, Libbrecht L, Hansen BE, Desombere I, Roskams T, Meuleman P, Leroux-Roels G. 2010. Factors determining successful engraftment of hepatocytes and susceptibility to hepatitis B and C virus infection in uPA-SCID mice. J Hepatol 53:468–476. https://doi.org/10.1016/j.jhep.2010.03.024.
43. Pas SD, de Man RA, Mulders C, Balk AH, van Hal PT, Weimar W, Koopmans MP, Osterhaus AD, van der Eijk AA. 2012. Hepatitis E virus infection among solid organ transplant recipients, the Netherlands. Emerg Infect Dis 18:869–872. https://doi.org/10.3201/eid1805.111712.